Title

The impact of agricultural managed aquifer recharge on the fate and transport of pesticides in the unsaturated zone

Authors

Zhou, Tiantian
Ruud, Nels
Šimůnek, Jiří
et al.

Publication Date

2024-09-01

DOI

10.1016/j.watres.2024.122442

Peer reviewed

The impact of agricultural managed aquifer recharge on the fate and transport of pesticides in the unsaturated zone

Tiantian Zhou[a,*], [illegible] Šimůnek[c], [illegible] Brunet[illegible]
Levintal[e], Cristina Prieto García[a], Helen E. Dahlke[a,*]

a Department of Land, Air and Water Resources, University of California, Davis, CA, 95616, USA
b Department of Pesticide Regulation, California Environmental Protection Agency, Sacramento, CA, USA
c Department of Environmental Scienc[illegible] Riverside, CA, 92521, USA
d Department of Civil Engineering, University of Calabria, Rende, Italy
e Zuckerberg Institute for Water Research, The Jacob Blaustein Institutes for Desert Research, Ben-Gurion University of the Negev, Sde Boker campus, 84990, Israel
Corresponding authors: Tiantian Zhou (tzhou035@ucr.edu; tiantianzhouonly@gmail.com); Helen Dahlke (hdahlke@ucdavis.edu)

Abstract

Groundwater aquifers worldwide [illegible] compounded by population growth, economic development, and climat[illegible] Managed aquifer recharge provides one tool to alleviate flood risk and re[illegible] groundwater. However, concerns grow that intentional flooding of [illegible] groundwater recharge, a practice known as Ag-MAR, may increase the leaching of pesticides and other chemicals into groundwater. This study employs a physical[illegible] based unsaturated flow model to determine the fate and transport of residues of four pesticide in three vadose zone profiles characterized by differing fractions of sa[illegible] (41%, 61%, and 84%) in California's Central Valley. Here, we show that the complex heterogeneity of alternating coarse and fine-grain hydrogeologic units controls t[illegible] transit times of pesticides and their adsorption and degradation rates. Unsatu[illegible] zones that contain a higher fraction of sand are more prone to support preferential

flow, higher recharge rates (+8%), and faster (42%) water fl
transport, more flooding-induced pesticide leaching (about 22%), as well as more salt
leaching correlating with increased r
Interestingly, considering preferential flow predicted higher degradation and retention
rates despite shorter travel times, attributed to the trapping of pesticides in immobile
zones where they degrade more effectively. The findings underscore the importance
of considering soil texture and structure in Ag-MAR
environmental risks while enhancing groundwater recharge. The study also highlights
that selecting less mobile pesticides can reduce leaching risks in sandy areas.

Keywords: HYDRUS, Particle swarm optimization, Preferential flow, Pesticide leaching; Capillary barrier

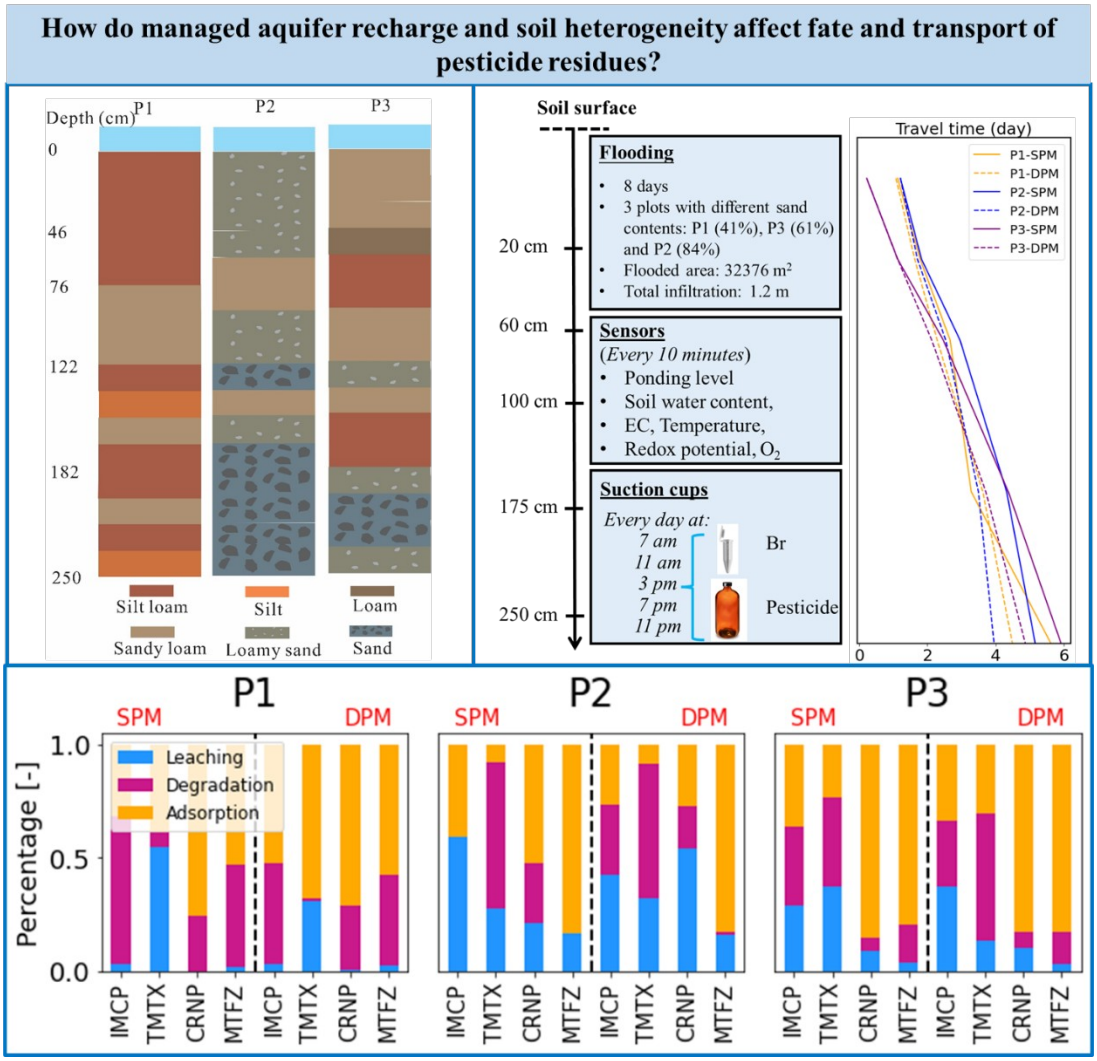

1 Introduction

California is leading the United States agricultural produ
different products including fruit, vegetable and specialty crops such as to
(70%), bell peppers (38% of
(Lucier. Iamn,id thaiJ qe hmr oea p
chlorantraniliprole and *methoxyfenozide* are common pesticides used to cultivate
many of these crops. Pesticides have played a substantial role in improving
yields, but also bear the risk of polluting freshwater resources w
harmful impacts on human health whe
(Tudi et al., 2021). Diffuse pesticide leaching from agricultural fields is the dominant
source of pesticides in streams and groundwater.

Pesticide management practices for runoff or groundwater protection areas have
been adopted in the US since the 1980; mandating for example minimum irrigation
amounts (6 – 25 mm) and banded applications to reduce surface runoff or leaching
risk to groundwater (EPA, 1987). The main processes controlling the fate
pesticides in the environment are degradation, rete
atmospheric dispersion, runoff, and leaching (Montiel et al., 2019). Once pesticides
enter the soil or vadose zone, their fate is controlled by adsorption to clay particles or
organic matter, transformation and degradation processes, soil water flow, and crop
uptake (Köhne et al., 2009).

While pesticide fate and transport has been studied at soil column to plot
catchment scales for decades, understanding their fate in natural or structured soils
has been a particular challenge since structured soils can
pesticides or other contaminants via non-equilibrium preferential flow pa
macropore flow) before they can degrade or be adsorbed. Most agricultural soils are
structured soils that contain various soil horizons with contrasting soil hydraulic or
chemical properties. In addition, agricultural soils receiving pesticide appli
often undergo a variety of natural processes (e.g. wetting-drying cycles, shrink-swell

behavior) and management practices (e.g. tillage, plowi
preferential flow.

Because structured soils are prone to preferential flow, pes
models (e.g. MACRO, HYDRUS, PEARL, DAISY, CR
PESTLIS, SIMULAT) that explicitly consider preferential flow have been shown to
outperform models (Köhne et al., 2009; Scorza and
2005). For example, Holback et al. (2022) used the agrohydrological model DAISY
to simulate the transport of bentazone and imidacloprid to drainpipes in a cracking
clay field. After incorporating preferential flow features such as biopores and cracks
into the model, it simulated satisfactorily water flow and pesticide leaching to drain
tiles (Holbak et al., 2022). Imig et al. (2023) observed the transport of four herbicides
(metolachlor, terbuthylazine, prosulfuron, and nicosulfuron) in two lysimeters filled
with a sandy gravel and clayey sandy silt over 4.5 years and simulated transport in
HYDRUS-1D. They found that pesticide transport could be adequately desc
using nonequilibrium (i.e. dual-porosity) models, where each model had a differently
sized mobile and immobile zones. For the clayey sandy silt the relativ
mobile zone was dominating solute transport, leading to higher solute concentration
in the column drainage (Imig et al., 2023a). Dusek et al. (2015) simulated the fate and
transport of five pesticides, including atrazine (quin, sulfomet
metolachlor, and imidacloprid) in undisturbed tropical Oxisol soi
experiment by considering (or not) chemical nonequilibrium in HYDRUS-1D. They
showed that atrazine, sulfometuron methyl, and S-metolachlor were better described
considering kinetic sorption, while the other two pesticides could be s
characterized using the chemical equilibrium model (Dusek et al., 2015). Sidoli et al.
(2016) investigated the fate and transport of metolachlor and its two metabolites in
column-leaching experiments in glaciofluvial soils, considering both physi
chemical nonequilibrium in HYDRUS-1D. They identified a strong in
chemical nonequilibrium on the fate of metolachlor b

(Sidoli et al., 2016). Köhne et al. (2006) applied multiple physical and nonequilibrium models in HYDRUS-1D to simulate the fate and transport of isoproturon, terbuthylazine, terburazine, and bromide in a aggregated loam columns subjected to multiple irrigation cycles. They showed that simultaneous consideration of preferential flow and kinetic adsorption (using the dual-permeability model with two-site sorption) provided the best model performance (Köhne et al., 2006).

Many studies to date have focused on pesticide leaching in agricultural soils under controlled conditions (e.g. soil column or lysimeter experiments) or natural precipitation or irrigation regimes to evaluate soil management practices for different soil types. These studies have resulted in pesticide best management practices such as pesticides with medium or high mobility should not be applied to saturated soils (Waskom, 1995). However, not many studies have focused on the fate and transport of pesticides under large water applications (> 150 mm [6 inches]), in coarse textured soils (e.g. soils that support large percolation rates), considering preferential flow and kinetic transformation processes (Pang et al., 2000). The study of pesticide fate under large water applications is of particular interest, as many groundwater-dependent agricultural regions (Perez et al., 2024), requiring managed aquifer recharge of depleted aquifers by using agricultural lands for both, agricultural production and managed aquifer recharge (MAR) (Dahlke et al., 2018; Levintal et al., 2023b). Agricultural managed aquifer recharge (Ag-MAR), where groundwater is actively replenished by spreading flood flows onto agricultural lands, may exacerbate the leaching of pesticide residues from the root zone to groundwater because of the large amounts of water (e.g. 0.5 to over 10 m of recharge) applied for MAR (Bachand et al., 2014; Guo et al., 2023; Levintal et al., 2023a; Murphy et al., 2021; Waterhouse et al., 2021). Detailed knowledge of the fate and transport of pesticides in the vadose zone of agricultural soils when flooded for MAR is needed to

adequately inform the placing of suitable Ag-MAR locations. Evidence that th
systems or conditions require more research can be gleaned from a few studies that observed early arrivals of pesticides at the groundwater table in response to strong precipitation or irrigation events soon after pesticides were applied in coarser, more heterogeneous materials (e.g., Cassel et al., 1995). Addressing this gap helps us assess the feasibility of implementing Ag-MAR while avoiding (or minimizing) groundwater pollution.

In this study, we combine field observations and non-equilibrium flow modeling in HYDRUS-1D to describe the fate and (*imidacloprid*, *thiamethoxam*, *chlorantraniliprole*, and *methoxyfenozide*) and bromide in the vadose zone of three Ag-MAR field sites in the Central Valley, Californi USA. Our main research objectives are 1) to capture and compare the transport of the four pesticides in three agricultural soils in response to one large (1.2 m) water application using water balance and mass balance approaches; 2) evaluate the role of vadose zone heterogeneity (e.g. soil hydraulic and chemical properties) on the occurrence of non-equilibrium preferential flow at the three sites and its impact on the water and contaminant (e.g., transport resistance); and 3) analyze sensitivity of solute transport and reaction parameters in HYDRUS, their calibration using global optimization methods, and how they related to dominant processes and factors governing the fate and transport of pesticides.

2 Methods

2.1 Study site and soil texture profiles

The Ag-MAR experiment was conducted at the Terranova Ranch (36°34'27"N 120°05'39"W, 50 m), located southwest of Fresno, CA, USA (Fig. 1a), within the Kings River basin, which is underlain by a predominantly sand and gravel aquifer bound by the Corcoran Clay at a depth of 140 m, a thick aquitard that spans th

western half of the Kings River basin. The depth of the groundwater t
approximately 70 meters at the time of data acquisition (February 2021).

The soil at the site is a Traver fine sandy loam (fine-loamy, mixed, ther
Natric Haploxeralf). Laboratory sediment analysis of undisturbed soil samples of the top 2.5 m of each soil profile (P1, P2, and P3) showed progressively inc
fractions of sand from P1 (41%) to P3 (61%) and
(Fig. 7 and Table S1), with a cemented duripan at around 1 m depth at P1 and P3
(Bachand et al., 2014).

2.2 Application of flood water, bromide tracer, and pesticides

A 32,376 m^2 (8 acres) recharge plot (Fig. 1b) was flooded in February 16-24, 2021, using pumped groundwater. A total of 38,774.74 m^3 of water (1.2 m in depth) was applied at a flow rate of ~3.35 m^3/min. The start times of flooding at each soil profile location were deduced from the time of water content increase, which was 12:50 on Feb. 16 at P3, 14:00 on Feb. 17 at P2, and 8:00 on Feb. 18 at P1. The end times of flooding at each soil profile were deduced from the endpoints of decreasing levels in surface ponding, which were 12:40 on Feb. 24 at P3, 19:50 on Feb. 24 at P2, and 19:50 on Feb. 24 at P1.

At each profile, 541 g of Br^- (838 g of KBr) dissolved in 100 L of water were applied. The area of the tracer application was 2.5 x 7 m^2 within each profile (Fig. 1c). The KBr solution was applied on February 15th, 2021, at P1 and P2, on February 16th, 2021, at P3, between 7:30-10 am. Br^- was thus applied at a concentration of 5410 ppm at an irrigation rate of 0.00381 cm/min.

Table S2 shows the history of pesticide applications and their rates for the four pesticides studied (*chlorpyrifos*, *dimethomorph*, *indoxacarb*, and *methoxyfenozide*). Table S3 provides the basic physical and chemical properties of these pesticides.

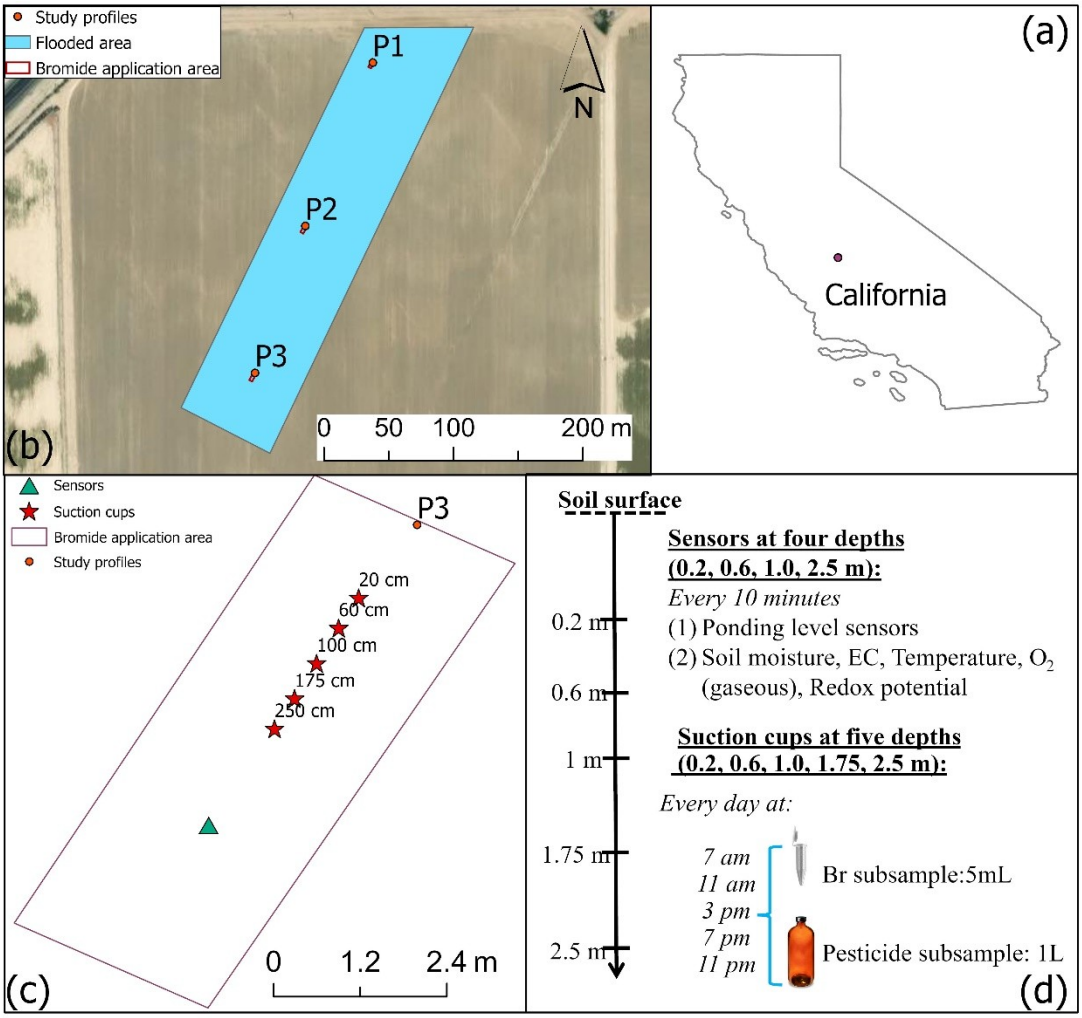

Fig. 1.A schematic of the study site in California, USA (a), the recharge plot, three soil profiles P1, P2, P3, and the potassium bromide (KBr) application location in each profile (b), sensors and suction cups in each profile (c), and sampling details (d).

2.3 Field monitoring and data collection

The meteorological data, including precipitation (P) and potential evaporation (E_p), were obtained from station 2 (Five Points (https://cimis.water.ca.gov/).

Sensors were installed at depths of 0.2, 0.6, 1.0, and 2.5 m at each soil profile. Sensors measuring ponding depth (CS-451, Campbell Scientific, Logan, UT, USA), soil water content, electrical conductivity (EC), and soil temperature (TEROS METER Inc., San Francisco, CA, USA), and gaseous O_2 (AF sensor KE-25, Figaro Sensors,

Rolling Meadows, IL, USA), and oxidation-reduction potential (ORP; built in house) were logged at a 10-minute time interval (Fig. 1c-1d).

Breakthrough curve data for the KBr tracer and pesticides were collected using high-volume dual-chamber suction cups (Model 1920 F1L24-B02M2, SoilMoisture Inc., Goleta, CA, USA), which were installed at depths of 20, 60, 100, 175, and 250 cm and sampled at 7:00, 11:00, 15:00, 19:00, and 23:00 every day during flooding. The suction cups were installed approximately 50 cm away from one another within a horizontal distance of (Fig. 1c-1d).

2.4 HYDRUS-1D model setup

Water flow and the transport of potassium bromide (KBr) and pesticides in the unsaturated zone were simulated using the single and dual-porosity models (SPM and DPM) of the HYDRUS-1D software (Šimůnek et al., 2016). SPM assumes that flow and transport processes in soil are uniform and can be described using the Richards and advection-dispersion equations, respectively. DPM divides the soil pore space into mobile and immobile regions (i.e., considering preferentia Water flow or solute transport occurs only in the mobile region, as described by the Richards and advection-dispersion equations, respectively. At the same time, there can be water/solute transfer between these two regions. The model setup, including input data, initial/boundary conditions and governing equations, is shown in Fig. 2 and Table S4. More details about the governing equations can be found in Text S1 (Supporting Information).

The 250 cm soil profile was divided into five modeling layers ranging from 0-46 cm, 47-76 cm, 77-122 cm, 123-182, and 183-250 cm by grouping the original soil texture of the profile (Table S1) and associating each model layer with one sensor depth (sensor installed at The simulation period was 104 days long, from 0:00 on Dec. 17, 2020, to 24:00 on

Mar. 31, 2021, which included pre-flooding, flooding (Feb. 16~Feb. 24, 2021), and post-flooding periods. The spatial discretization was 1 cm throughout the soil profile, while the temporal discretization was variable, with a minimum time step of 0.0 minutes.

The initial soil pressure head profile was obtained from measured soil wa contents at four soil depths (20, 60, 100, and 250 cm) and soil water retention curves of typical soil textures (Radcliffe and Šimůnek, 2018) linearly interpolated between any Br^- concentrations were set to zero throughout the soil profile, while the initial soil water pesticide concentrations were prescribed based on field measurements.

For water flow, the upper boundary condition (BC) was set to an atmospheric flux (with a maximum allowed surface water layer of 50 cm, i.e., the height of the berms). The potential water flux across the soil surface is the difference between daily values of potential evaporation (E_p) and precipitation (P) atmospheric (and irrigation (F). The lower BC at the soil depth of 250 cm was set to free drainage because of the low water table at the site the upper BC was prescribed as a solute flux (i.e., a Cauchy BC), with bro concentrations and irrigation fluxes during the bromide application as inputs. model then automatically adjusts surface bromide concentrations depending on the depth of the surface water level, evaporation, precipitation, irrigation fl associated bromide concentrations. The lower BC was p concentration gradient (i.e., a Neumann BC when only a convective s occurs).

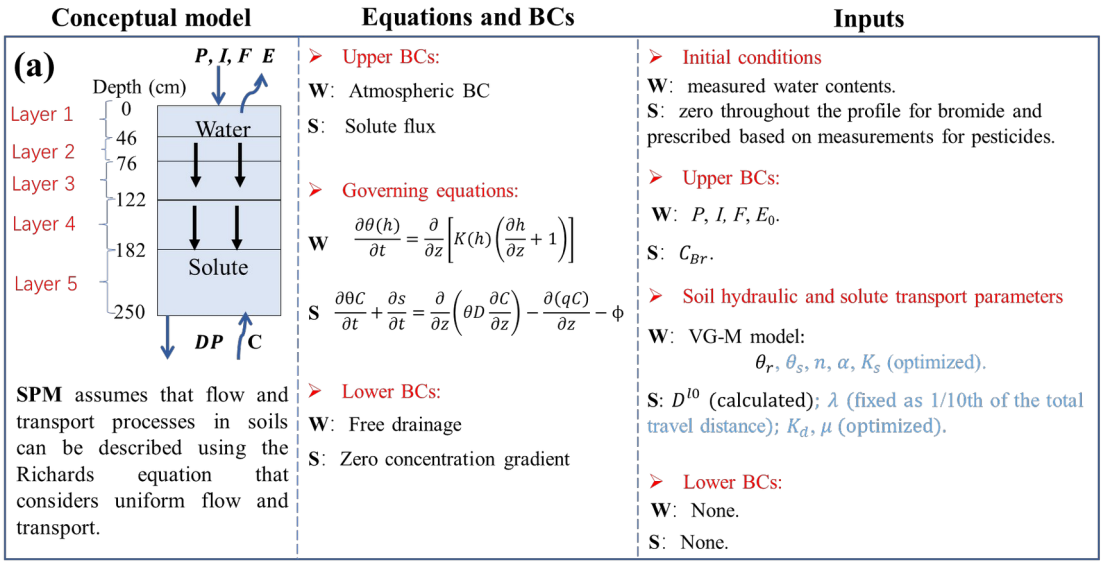

246

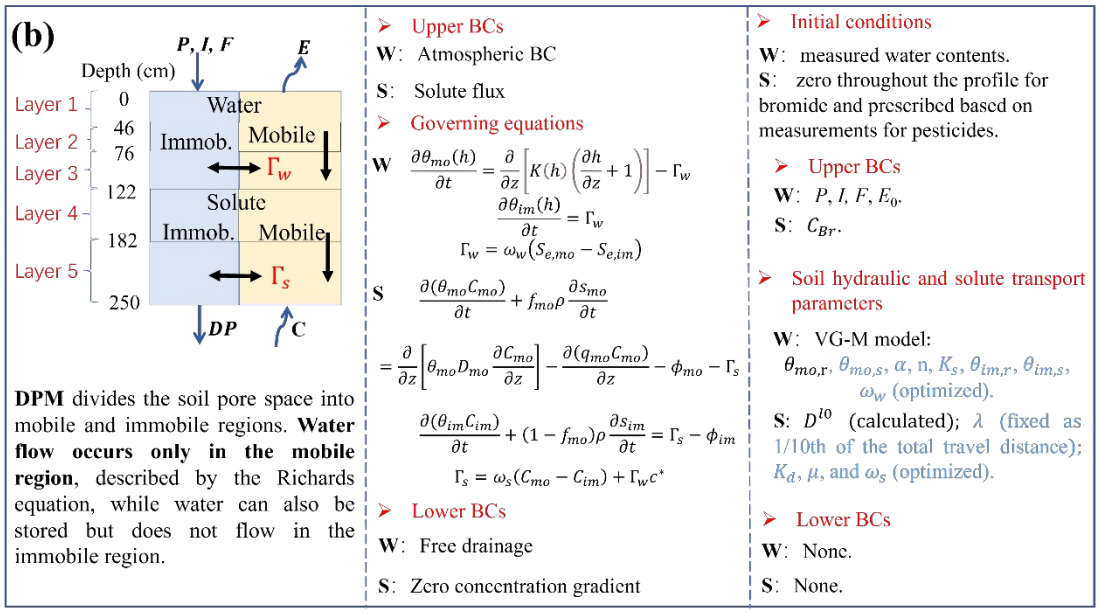

247

248 Figure 2 Conceptual model setups for the (a) single-porosity and (b) dual-porosity
249 models (SPM and DPM, respectively). Note that "W" and "S" represent water flow
250 and solute transport, respectively. The explanations of each variable are shown
251 Supplemental materials S1.
252

253 **2.5 Parameter optimization and sensitivity analysis**

254 In this study, we adopted a two-step optimization. Since bromide transport is
255 largely unaffected by adsorption/desorption and degradation, measured breakthrough
256 curves (BTCs) of bromide were used first to estimate the soil hydraulic and basic

(e.g., dispersivity) solute transport parameters for both the single and dual-porosity models.

In the single-porosity models, θ_r was not optimized. Instead, the default values of corresponding soil textures were adopted first and then manually adjusted to obtain a better model fit. Therefore, five parameters (θ_s, α, n, K_s, and λ) were optimized for each layer (25 parameters in total). The ranges of other parameters (Table S5) were prescribed as 1/5th and 6/5th of the minimum and maximum of their initial values for all soil textures in each modeling layer, obtained from the Ro HYDRUS-1D, based on measured soil textural data (Table S1).

To reduce the number of optimized parameters in the dual-porosit $\theta_{m,r}$ was set to zero, as done in many similar studies (Haws et al., 2005; Šimůnek et al., 2001). Therefore, eight parameters ($\theta_{mo,s}$, α, n, K_s, $\theta_{\mathfrak{Z},r}$, $\theta_{\mathfrak{Z},s}$, ω_w, and λ) were optimized for each layer (40 paramet α, n, K_s, and λ (Table S7) were the same as those in the single-porosity models. The upper boundary of $\theta_{mo,s}$ and $\theta_{\mathfrak{Z},s}$ were the same as ranges of θ_s in the single-porosity models, while the lower boundary was set as 0.1 and 0.01, respectively. The ranges of $\theta_{\mathfrak{Z},r}$ and ω_w (Table S7) were set (1.0e-01 and 2.0e-03) ~ 7e-3 min^{-1} (Brunetti et al., 2016), respectively.

In the second step, the parameters θ_r, α, n, K_s, and λ in the single-porosity model of $\theta_{mo,s}$, α, n, K_s, $\theta_{\mathfrak{Z},r}$, $\theta_{\mathfrak{Z},s}$, ω_w, and λ in the dual-porosity model obtained during the first step were fixed, while the (i.e., adsorption and degradation) were optimized based on measured pesticide BTCs. In this second step, nonequilibrium was n two parameters (K_d and μ) were optimized for each layer (10 parameters in total) in the single-porosity model, while three parameters (K_d, μ, and ω_s) were optimized for each layer (15 paramet model. Measurements of degradation or sorption parameters specific to the study site were unavailable. The ranges of K_d (Tables S6 and S8) were prescribed as 0 and 6/5

times the maximum K_{oc}*TOC (i.e., the total organic carbon content) for all soil textures in each modeling layer (Tables S1 and S3). The ranges of μ (Tables S6 and S8) were prescribed as 0 an ln2/$t_{1/2}$ for all soil textures in each modeling layer (Table S3). Th ω_s (Table S8) were set to 0~7e-3 min^{-1} (Imig et al., 2023a).

The parameter optimization was performed using the par optimization (PSO) algorithm using the PySwarm Library in Python. A swarm of candidate solutions is moved around in the search space in the PSO according to a few equations. The movement of the particles is guided by their optimal positions and that of the whole swarm. Once improved positions are discovered, they guide th swarm's movement. This process is repeated until the global optimal position that all particles tend to follow is found (Shi and Eberhart, 1998). More details about PSO can be found in (Brunetti et al., 2016) (Brunetti et al., 2017; Brunetti et al., 2022; Zhou et al., 2022).

The PSO parameters (cognitive parameter c_1=0.2677; social parameter c_2=3.395; inertia-weight w=0.4440 (Brunetti et al., 2016)) were used in this study. The number of swarm particles and iterations is 200; optimization had 40,000 runs. The Python script produces an input parameter space, overwrites the input parameter file, and runs the executable module of HYDRUS-1D. For each PSO run for the water fl parameters, the Kling-Gupta efficiency (KGE) indices for the dynamics of surface ponding levels (KGE_sp), soil water co concentrations (KGE_avg=0.7*KGE_wc+0.2*KGE_sp+0.1*KGE_B determined based on the degree of trust in these three types of data) were calculated. For each PSO run for the p parameters, the Kling-Gupta efficiency (KGE) indices for pesticide concentrations (i.e., KGE_Imi, KGE_Thi, KGE_Bo ...

KGE (*Methoxyfenozide*) were calculated. The KGE index compares the correlation coefficient (r), the ratio of means (β), and the ratio of variability (γ) between simulated and observed data (Knoben et al., 2019). The value of the KGE index is always smaller or equal to 1. The higher the KGE value, the better the fit between the simulated and observed values.

$$KGE = 1 - [(1-r)^2 + (1-\beta)^2 + (1-\gamma)^2]^{0.5} \quad (22)$$

If a HYDRUS-1D run was not completed within the time limit (i.e., 60 s for the single-porosity models and 600 s for the dual-porosity models) or the length of the modeled hydrograph was shorter than the total simulation period (149,760 minutes), the run was considered non-convergent. The run was then terminated, and a large negative value (i.e., -1.0E+07) for the objective function. Only the parameters leading to the maximum KGE_avg were retained as optimized parameters.

The Sobol' global sensitivity analysis using the Sensitivity Analysis Library (SALib) interface in Python to identify the most influential transport and reaction parameters of pesticides (Text S2).

3 Results

3.1 Model parameters and performance

The HYDRUS-1D single-porosity (SP) and dual-porosity (DP) transport models were first fit to the observed volumetric water contents, ponding depths, and KBr tracer breakthrough data before pesticide adsorption and degradation parameters were optimized. With a few exceptions, the optimized soil hydraulic parameters (Tables S4-S5) fell within the typical ranges of other studies (Text S1). Although all three Ag-MAR sites were classified as Traver fine sandy loam, the P1 and P3 sites exhibited a clear cemented duripan at 77-122 cm depth (Bachand et al., 2014) which resulted in lower

(K_s) at these depths (about 0.022 cm/min). In general, K_s values were largest at P2, the sandiest profile of the three (84% sand), and lowest at P1 (41% sand), while P3 (61% sand) was in between the two. Optimized adsorption coefficients for the pesticides (Tables S4-S6) were largest at P1 and lowest at P2, following the pattern of their total organic matter contents (Fig. 7). In contrast, *chlorantraniliprole* and *methoxyfenozide* had relatively high adsorption but lower degradation coefficients than *imidacloprid* and *thiamethoxam*, indicating that they were less mobile and more persistent in the environment.

The observed surface ponding levels (Fig. 3) quickly increased to their maximum (about 11 cm, 12 cm, and 21 cm in profiles P1, P2, and P3, respectively) because of continuous flooding. After that, the ponding level decreased when water application stopped. The water contents at all depths (Fig. 4) exhibited increasing trends during the flooding period and decreased during the post-flooding period.

The bromide BTCs at all depths (Fig. 5) first showed increased concentrations, followed by decreased concentrations with time. The P2 profile overall had the lowest concentrations, the fastest arrival rates of peak concentrations during flooding, and the least pronounced tailing of BTCs. In contrast, the P1 profile had the highest concentrations, the slowest arrival times of peak concentrations after flooding started, and the most pronounced tailing of BTCs.

Most pesticide BTCs (Fig 6 and Figs. S1-S3) showed reduced concentrations in the surface layers due to leaching, except for *methoxyfenozide*, which increased in concentration at 20 cm due to the pesticide transfer from the topmost layer. However, changes in pesticide concentrations within the deeper layers varied a lot, from rising (mostly at P1), falling (mostly at P2), or initially rising before falling (mostly at P2 and P3). These patterns indicate different arrival rates of peak pesticide concentrations during flooding: slowest at P1, fastest at P2, and medium at P3.

In the single-porosity models (SPM) fitted to the BTCs, simulated wetting fronts progressively arrived later at increasing depths than those observed, especially at P2 and P3. Similar to wetting fronts, simulated bromide breakthroughs arrived later than those observed at depths at P2 and P3. The simulated bromide BTCs also had larger tailings than those observed. There was a mismatch between pesticide modeled simulations and observations. These may suggest the presence of preferential flow/transport at P2 and P3 due to the occurrence of mobile and immobile zones and the solute mass transfer between them. Due to fast water movement during flooding, mixing with immobile water is limited. As a result, solute mixing occurs mainly within the available water (Imig et al., 2023b), leading to higher observed solute concentrations and less tailing than simulated by SPM at P2 and P3. This also highlights the potential utility of applying a weighted nonlinear least squares (e.g., Gan et al., 2009; Lamba et al., 2020) which allows for specifying the relative importance of components (i.e., correlation, variability bias, and mean bias between observed and simulated values) to better capture solute arrivals (Table 1).

The dual-porosity models (DPM) improved the model performance in simulating surface ponding levels, water contents, and bromide BTCs at P1, but worsened it for pesticide BTCs. DPMs improved the model performance in simulating ponding levels and bromide, and *chlorantraniliprole* BTCs at P2. However, it worsened the model performance in simulating soil water contents and the *thiamethoxam* and *chlorantraniliprole* BTCs. DPMs improved the model performance at P3 in simulating surface ponding levels, bromide, *imidacloprid*, and *methoxyfenozide* BTCs. However, it worsened it for soil water contents and *thiamethoxam* and *chlorantraniliprole* BTCs. In other words, the model performance in simulating the bromide and pesticides BTCs cannot be improved simultaneously, and it can even be worsened when switching from SPM to DPM.

This may be because the solute transport parameters were optimized for bromide BTCs and thus may not apply to pesticide BTCs.

Overall, SPM and DPM could not adequately describe the observed surface ponding levels, soil water contents, and bromide/pesticide BTCs (Table 1). Köhne et al. (2009) compared different pesticide transport models and concluded that a model gives satisfactory predictions if the ratio between measured and modeled concentrations is less than 3-5 (Köhne et al., 2009). The ratio was generally less than 3 in this study, indicating that the fit was fairly adequate. The performance for *bromide*, *thiacloprid*, *dimethoxam*, and *chlorantraniliprole* was much better than for *orthoxyfenozide*. This may be related to the omission of potential chemical nonequilibrium in this study since rapid water flow (Dusek et al., 2015).

Surface ponding level

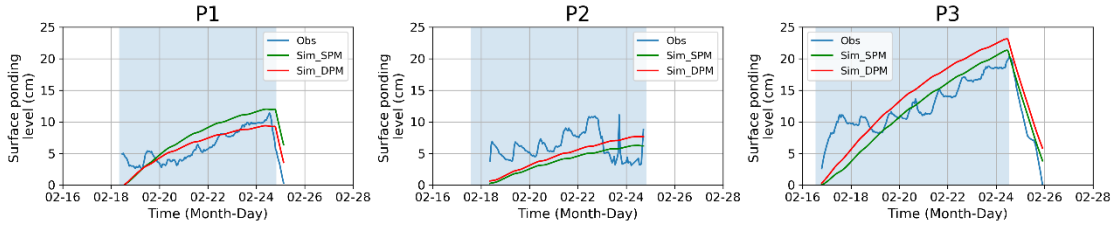

Figure 3. Observed and simulated (using the single-porosity [SPM] and dual-porosity [DPM] models) surface ponding water levels in the three soil profiles P1, P2, and P3 (left to right). The blue-shaded areas indicate the flooding period.

Water content

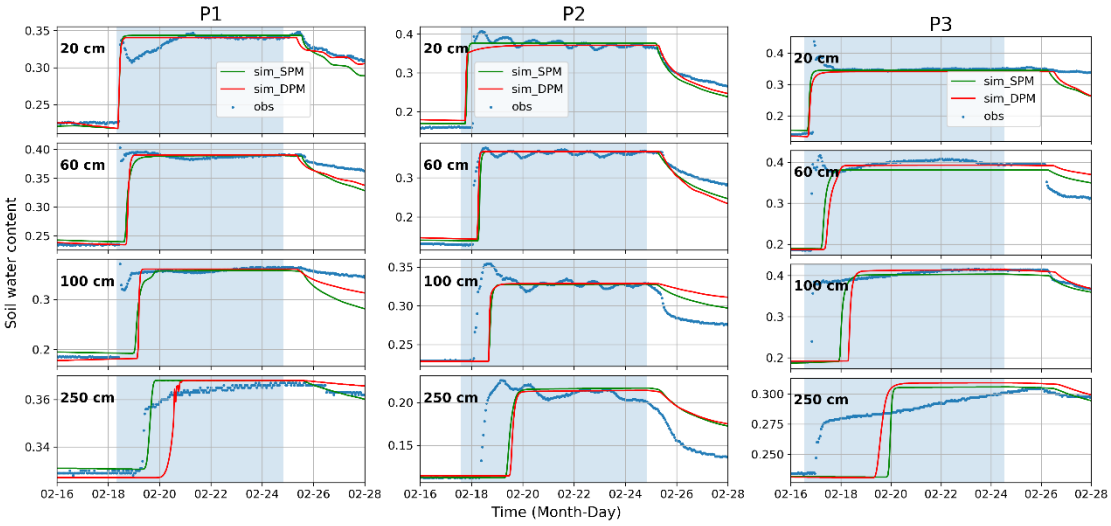

Figure 4. Observed and simulated (using the single-porosity [SPM] and dual-porosity [DPM] models) soil water contents at different depths (20, 60, 100, and 250 cm; top to bottom) in the three soil profiles P1, P2, and P3 (left to right). The blue-shaded areas indicate the flooding period.

Bromide

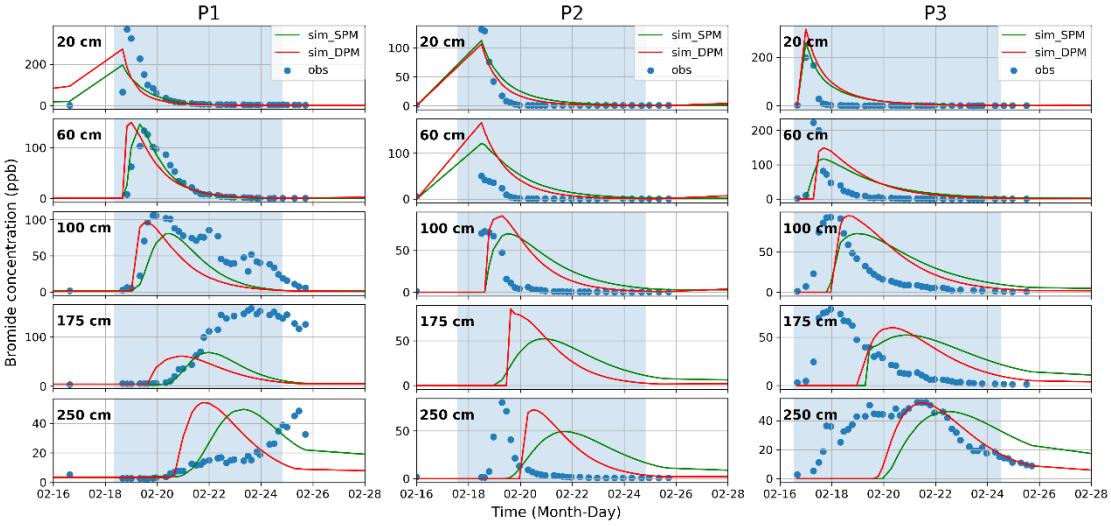

Figure 5. Observed and simulated (using the single-porosity [SPM] and dual-porosity [DPM] models) bromide concentrations at different depths (20, 60, 100, and 250 cm; top to bottom) in the three soil profiles P1, P2, and P3 (left to right). The blue-shaded areas indicate the flooding period.

Imidacloprid

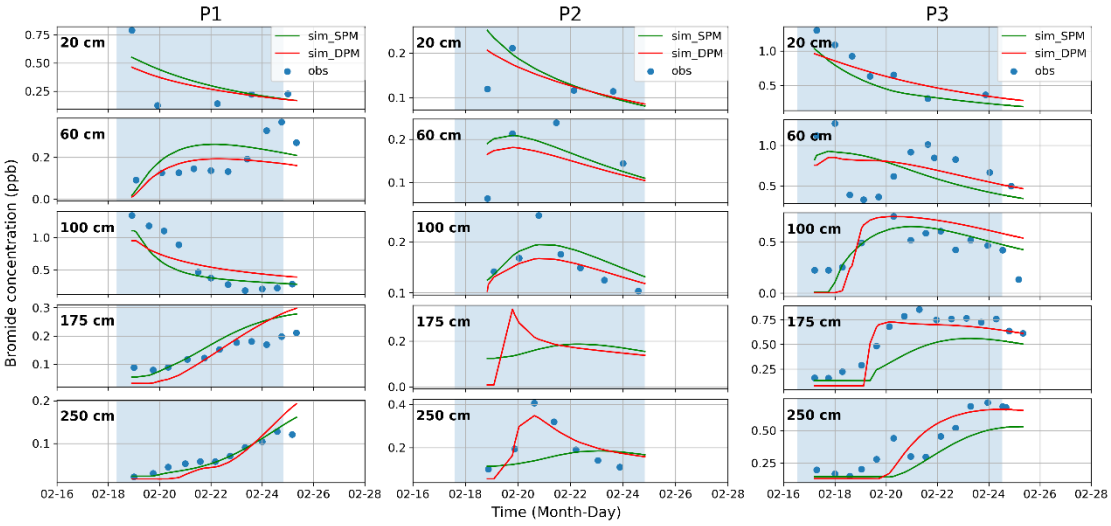

Figure 6. Observed and simulated (using the single-porosity [SPM] and dual-porosity [DPM] models) *imidacloprid* concentrations at different depths (20, 60, 100, and 250 cm; top to bottom) in the three soil profiles P1, P2, and P3 (left to right). The blue-shaded areas indicate the flooding period.

Table 1. Model performance (Kling-Gupta Efficiency) of the single-porosity [SPM] and dual-porosity [DPM] models to simulate surface ponding levels, soil water contents, and concentrations of bromide and four pesticides (*imidacloprid*, *thiamethoxam*, *chlorantraniliprole*, and *methoxyfenozide*) in the three soil profiles (P1, P2, and P3).

Variable	P1		P2		P3	
	SPM	DPM	SPM	DPM	SPM	DPM
Surface ponding level	0.67	0.76	0.02	0.1	0.44	0.6
Water content	0.87	0.89	0.94	0.93	0.83	0.8
Bromide	0.44	0.38	-0.69	-0.38	0.27	0.3
Imidacloprid	0.78	0.73	-0.08	0.7	0.7	0.73
Thiamethoxam	0.67	0.59	0.68	0.66	0.7	0.65
Chlorantraniliprole	0.81	0.56	0.24	0.31	0.89	0.75
Methoxyfenozide	0.65	0.58	0.2	0.14	0.81	0.85

3.2 Water mass balances and travel time of flooding water

The water balance and recharge amounts estimated with the SPMs and DPMs showed distinct differences with Table)2Groundwater recharge was largest at P2 (SPM: 89.7%, DPM: 90. smallest at P1 (82.6%, 83.4%), and intermediate (but close to P1) at P3 (83

83.6%).The water mass balance varied by up to 8% between P2 and the other two profiles.

Considering preferential flow by DPMs resulted in lower bromide travel times by up to 23% and higher flow velocities by up to 31% compared to SPM expected, the sandiest profile P2 had the highest flow velocity, followed by P1, while P3 had the lowest. Accordingly, transport velocities between the th profiles differed by about 42 %, ranging between 16.54 and 91.84 cm/day in the 2.5 m near-surface unsaturated zone (Fig. 7, Table 3).

3.3 Pesticide mass balance

Among the sites, P2 showed t (L_p) with an average of 37.5%, followed by P3 at 19.4%, and P1 at 12.2%. The DPM model predicted slightly higher leaching (1.8% on average) compared to the SPM model, with P2 experiencing approximately 21.6% more leaching than the other sites on average. *Imidacloprid* and *thiamethoxam* had significantly higher leaching rates, averaging 22.3% more than *chlorantraniliprole* and *methoxyfenozide* (Fig. 7, Table 4).

With respect to degradation (D_p), P1 had the highest degradation rate, averaging 31.9%, while P2 and P3 were at similar levels (27.7% and 26.6%, respectively). The DPM model predicted about 2.7% more degradation on average than the SPM, with P1 showing a 4.8% higher de *Imidacloprid* and *thiamethoxam* also degraded more, with an average of 19.1% higher than *chlorantraniliprole* and *methoxyfenozide* (Fig. 7, Table 4).

In terms of retention ($S_{p,final}$), P1 and P3 retained the most (averaging 56.1% and 57.9%, respectively), while P2 retained the least (43.2%). Retention was about 3.8% higher in the DPMs than in the SPMs, with P1 and P3 showing an average of 8.2% more retention than P2. *Chlorantraniliprole* and *methoxyfenozide* exhibited greater

retention in the soil, averaging 33.9% more than *imidacloprid* and *thiamethoxam* (Fig. 7, Table 4).

Regarding changes in pesticide storage ($\Delta S_{p,RZ}$ and $\Delta S_{p,DVZ}$), *imidacloprid* and *thiamethoxam* in general lost significant amounts of pesticides from both the root zone and deep vadose zone, while *chlorantraniliprole* and *methoxyfenozide* typically showed losses in the root zone but gains in the deep vadose zone (Fig. 7, Table 4).

Overall, P1 and P3 showed more retention or degradation, while P2 exhibited greater leaching. These findings are supported by the fact that the adsorption degradation coefficients were largest at P1, followed by P3, while they were lowest at P2, as discussed in Section 3.1. Furthermore, the DPMs generally show leaching, degradation, and retention than the SPMs

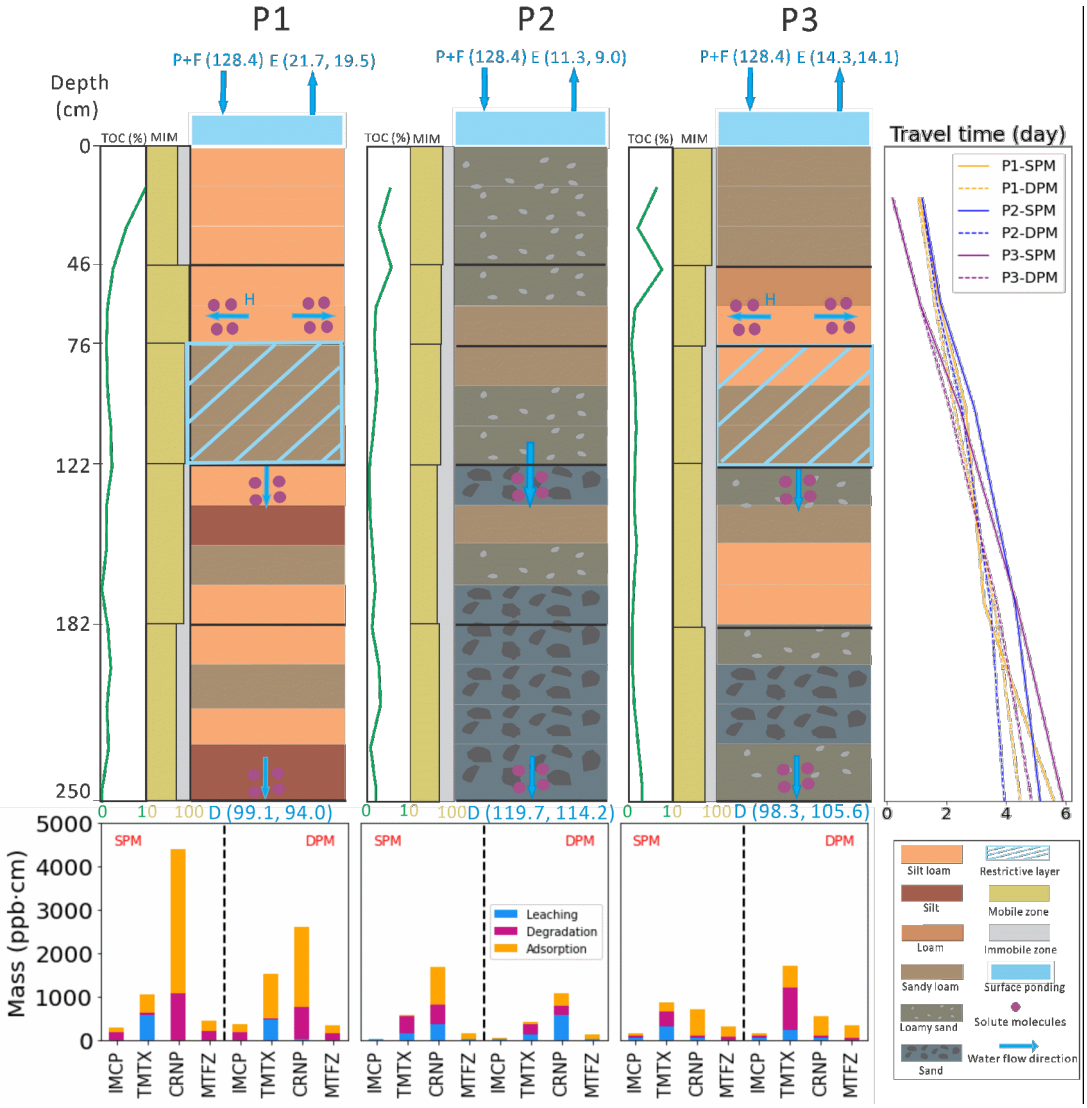

Figure 7. Conceptual model of flow and pesticide transport processes, water and pesticide mass balances, and bromide travel times during Ag-MAR in the top 2.5 m of the three soil profiles (P1, P2, and P3). F: Flooding; E: Evaporation; H: horizontal flow caused by a capillary barrier; D: Deep drainage. The two numbers to the right of these terms are water mass amounts (in cm) calculated using the single-porosity (SPM) and dual-porosity (DPM) models. The bottom bar plots show adsorption, degradation, and leaching amounts (in ppb.cm) for the four pesticides, including *imidacloprid* (IMCP), *thiamethoxam* (TMTX), *chlorantraniliprole* (CRNP), and *methoxyfenozide* (MTFZ), at the end of the simulations. TOC and MIM represent the total organic carbon content (%) and Mobile-Immobile zones, respectively.

Table 2. Water mass balance components for the three soil profiles P1, P2, and P3 calculated using the SPMs and DPMs.

Term	P1					P2					P3				
	SPM		DPM		Difference	SPM		DPM		Difference	SPM		DPM		Difference
	cm	%	cm	%	(%)	cm	%	cm	%	(%)	cm	%	cm	%	(%)
P+I	128.4		128.4			128.6		128.6			128.4		128.4		
E	21.7	16.9	19.5	15.2	-1.7	11.3	8.8	9.0	7.0	-1.8	14.3	11.1	14.1	11.0	-0.1
D	99.1	77.2	94.0	73.2	-4.0	119.7	93.1	114.2	88.8	-4.3	98.3	76.6	105.6	82.2	5.6
ΔS_{RZ}	4.6	3.6	4.4	3.4	-0.2	5.7	4.4	7.6	5.9	1.5	10.6	8.3	11.1	8.6	0.3
ΔS_{DVZ}	6.9	5.4	13.1	10.2	4.8	-4.3	-3.3	2.6	2.0	5.3	9.0	7.0	1.7	1.3	-5.7
GR	106.0	82.6	107.1	83.4	0.9	115.4	89.7	116.8	90.8	1.1	107.3	83.6	107.3	83.6	0

P: precipitation, F: flood irrigation, E: evaporation, D: drainage, ΔS_{RZ}: storage change in the root zone 0~100 cm, ΔS_{DVZ}: storage change in the deep vadose zone 100-250 cm, GR: groundwater recharge including D and ΔS_{DVZ} (since water flow is considered one-dimensional, deep drainage below the root zone will eventually recharge groundwater) (de Vries and Simmers, 2002).

Table 3. Travel times and average velocities of bromide (calculated by the peak displacement method) from the soil surface to different soil depths at three soil profiles P1, P2, and P3 calculated using the SPMs and DPMs.

Term	Depth (cm)	P1			P2			P3		
		SPM	DPM	Relative difference (%)	SPM	DPM	Relative difference (%)	SPM	DPM	Relative difference (%)
Travel time (day)	20	1.13	1.08	-4.4	1.21	1.21	0	0.22	0.22	0
	60	1.79	1.63	-8.9	1.83	1.71	-6.6	1.13	1.13	0
	100	2.67	2.29	-14.2	2.96	2.54	-14.2	2.47	2.13	-13.8
	175	3.29	3.63	10.3	4.33	3.5	-19.2	4.38	3.72	-15.1
	250	5.63	4.5	-20.1	5.17	3.96	-23.4	5.93	4.88	-17.7
Flow velocity (cm/day)	20	17.71	18.53	4.6	16.54	16.54	0	91.84	91.84	0

60	33.54	36.83	9.8	32.8	35.1	7	53.2	53.2	0
100	37.46	43.68	16.6	33.79	39.38	16.5	40.52	47	16
175	53.2	48.22	-9.4	40.42	50.01	23.7	39.97	47.07	17.8
250	44.41	55.57	25.1	48.36	63.14	30.6	42.17	51.25	21.5

Note that the peak displacement method estimates tr
(flooding) and output (different soil depths) of bromide BTCs (Zhou et al., 2023).

Table 4. Solute mass balance components for the four pesticides at the three soil profiles P1, P2, and P3 calculated using the SPMs and DPMs.

Pesticide	Term	P1					P2					P3				
		SPM		DPM		Difference	SPM		DPM		Difference	SPM		DPM		Difference
		ppb·cm	%	ppb·cm	%	%	ppb·cm	%	ppb·cm	%	%	ppb·cm	%	ppb·cm	%	%
Imidacloprid	$S_{p,init}$	280.2		363.6			31.6		33.1			147.2		117.68		
	L_p	9.5	3.4	10.8	3.0	-0.4	18.8	59.5	23.2	71.4	15.1	42.9	29.1	55.8	47.4	18.3
	D_p	180.9	64.6	161.6	44.4	-20.2	0	0.0	17.0	51.4	54.7	51.0	34.6	43.1	36.6	2.0
	$S_{p,final}$	89.0	31.8	189.7	52.5	20.7	12.8	40.5	14.5	43.8	6.1	53.4	36.3	50.3	42.7	6.4
	$\Delta S_{p,R}$	-120.5		-118.6			-18.2		-16.8			-102.1		79.0		
	$\Delta S_{p,D}$	-70.7		-55.3			-0.6		-1.9			8.3		11.6		
Thiamethoxam	$S_{p,init}$	1052.8		1527.8			592.8		421.7			874.9		1643.9		
	L_p	576.0	54.7	471.0	30.8	-23.9	164.0	27.7	132.0	31.3	3.6	328.5	37.5	234.6	14.3	-23.3
	D_p	69.0	6.6	17.3	1.1	-5.5	382.7	64.6	244.2	57.9	-6.7	340.7	38.9	963.4	58.6	19.7
	$S_{p,final}$	409.6	38.9	1032.7	67.6	28.7	45.0	7.6	35.6	8.4	0.8	206.3	23.6	517.4	31.5	7.9
	$\Delta S_{p,R}$	-232.0		-309.7			-136.1		-92.6			-303.4		182.7		
	$\Delta S_{p,D}$	-411.1		-185.5			-411.7		-293.5			-365.1		-666.5		
Chlorantraniliprole	$S_{p,init}$	4394.0		2599.6			1689.4		1054.9			702.9		561.6		
	L_p	8.8	0.2	23.1	0.9	0.7	362.4	21.5	581.0	55.1	33.6	65.7	9.3	58.1	10.4	1.1
	D_p	1073.4	24.4	730.7	28.1	3.7	448.2	26.5	206.8	19.6	-6.9	39.1	5.6	39.8	7.1	1.5
	$S_{p,final}$	3304.1	75.2	1844.7	71.0	-4.2	879.2	52.0	289.9	27.5	70.3	598.4	85.1	460.6	82.0	-3.1
	$\Delta S_{p,R}$	-1035.3		-681.1			-861.2		-244.0			-181.0		-162.6		
	$\Delta S_{p,D}$	-54.7		-73.8			51.0		479.0			76.4		61.7		

Methoxyfenozide	$S_{p,init}$	440.0		336.4			170.4		120.7			326.4		344.8		
	L_p	7.4	1.7	9.8	2.9	1.2	29.1	17.1	19.3	16.0	-1.1	13.2	4.0	12.0	3.5	-0.5
	D_p	200.4	45.5	137.1	40.8	-4.7	0	0.0	1.7	1.4	1.4	55.1	16.9	48.7	14.1	-2.8
	$S_{p,final}$	232.1	52.8	198.5	59.0	6.2	141.3	82.9	99.9	82.8	-0.1	258.2	79.1	285.4	82.8	3.7
	$\Delta S_{p,R.}$	-103.0		-69.3			-32.6		-24.6			-75.8		-65.2		
	$\Delta S_{p,D}$	-104.9		-68.5			3.5		3.8			7.6		5.7		

Note that S_{init} and S_{final} are the initial and final pesticide storages in the soil profile, respectively, L_p is the pesticide mass leached through drainage, D_p is the pesticide mass degraded through chemical or biological reactions, and ΔS_p is pesticide storage change in the root zone 0~100 cm ($\Delta S_{p,RZ}$) and deep vadose zone 100-250 cm ($\Delta S_{p,DVZ}$).

3.4 Model sensitivity analysis

The Sobol' global sensitivity analysis was conducted to identify the most influ parameters controlling the transport and reaction of pesticides within the SPMs (Table 5 and Text hSe2).r.eaTc t i o n p a r a m e t e r s (e s (K_d) of Layer 1 (the surface layer) were the most influential parameters in si *chlorantraniliprole* at all three profiles and *imidacloprid* at P2. This finding underscores the critical role that organic matter in the surface layer plays in the adsorption of pes which, in turn, affects their movement through the soil (Fig. 2). In addition to the surfac layer's role, the degradation (μ) parameter of Layer 3 (the restrictive layer where c e m e n t e d d u w i a p s a n h e c m o r s t i m p a c t f u l p *imidacloprid*, *thiamethoxam*, and *methoxyfenozide* at P1 and P3. This is likely because the presence of a restrictive layer at P1 and P3 increased the residence time of the infiltratin water and the potential for degradation. This finding again validates the conclusion that P1 and P3 show more retention or degradation, while P2 show more leaching, as discussed in Section 3.3.

Table 5. The most influential soil layers and reaction parameters (adsorption coefficient K_d; degradation coefficient μ) for modeling (using the single-porosity [SPM]) of four pesticides (*imidacloprid*, *thiamethoxam*, *chlorantraniliprole*, *methoxyfenozide*) at the three soil profiles (P1, P2, and P3).

Profile	P1		P2		P3	
Pesticide	Layer	Parameter	Layer	Parameter	Layer	Parameter
Imidacloprid	3	μ	1	K_d	1	μ
Thiamethoxam	3	μ	5	μ	3	μ
Chlorantraniliprole	1	K_d	1	K_d	1	K_d
Methoxyfenozide	3	μ	3	μ	1	μ

4 Discussion

4.1 Impacts of preferential flow on pesticide fate and transport

Preferential flow paths were more pronounced in the sandier profiles, such as P2 and P3, as indicated by the earlier arrival of observed water and solute fronts concentrations, and narrower bromide and pesticide BTC *imidacloprid* and *chlorantraniliprole* at P2 and *thiamethoxam* at P3) (Figs. 5-6 and Figs. S1-S3). Preferential flow led to faster water flow (Table 3), more groundwater recharge (Table 2) and more pesticide leaching (Table 4) in the unsaturated zone at P2 and P3, especially for more mobile pesticides like *imidacloprid* and *thiamethoxam*. The possible mechanisms that caused preferential wa (Zhou et al., 2023).

Interestingly, considering preferential flow using the dual-porosity predicted higher degradation and retention rates even though they showed sh times. This is because DPMs account for the unique interaction b immobile regions in the soil. In DPMs, pesticides can move quickly through the regions, but a significant portion gets temporarily trapped in the immobile regions, where the water is largely stagnant. This trapping allows pesticides to stay in contact with the soil for longer periods, which enhan (Ray et al., 2004).

4.2 Impacts of lateral flow on pesticide fate and transport

In addition to preferential flow, lateral flow also played a crucial rol transport, especially in profiles P1 and P3. The cm^3/cm^3 at P1 and 0.05 cm^3/cm^3 at P3, Fig. 4) in the deeper soil layers indicate unsaturated soil conditions. These unsaturated conditions below the duripan and notably higher pesticide concentrations at 100 cm than in the 60 cm (Fig. 6 and Figs. S1 - S3) in P1 and P3 profiles could potentially be related to the restrictive layer forming a capi barrier that promotes lateral flow within the low-conductivity layer to the overlying coarser-

558 textured soil layers (Fig. 7). This lateral flow led to the perching of water and pesticides at
559 specific depths (Zhu et al., 2023), particularly affecting less mobile pe
560 *chlorantraniliprole* and *methoxyfenozide*, which exhibited higher degradation and retention
561 than other two pesticides (Table 4). This is also supported by the sensitivity analysis results
562 which indicate that the degradation coefficient of the restrictive layer is a key factor in the
563 behavior of less mobile pesticides like *chlorantraniliprole* and *methoxyfenozide* in profiles P1
564 and P3 (Table 5).

565 **4.3 Differences in pesticide behavior**

566 Our results reveal distinct differences in the behavior of the four pesticides studied—
567 *imidacloprid*, *thiamethoxam*, *chlorantraniliprole*, and *methoxyfenozide*—highlighting the
568 importance of both chemical properties an
569 *Imidacloprid* and *thiamethoxam* were more mobile (more prone to leaching as seen in Table
570 4) than *chlorantraniliprole* and *methoxyfenozide*, consistent
571 (Tingle et al., 2003). Because of this, *imidacloprid* and *thiamethoxam* were significantly
572 affected by preferential flow, particularly in the sandier P2 profile (discussed in Section 4.1).
573 Conversely, *chlorantraniliprole* and *methoxyfenozide*, which are less mobile, were more
574 influenced by soil heterogeneity and lateral flow, leading to greater retention and degradation
575 in profiles with finer textures and more organic matter, such as P1 and P3 (discu
576 Section 4.2). The DPMs' ability to capture these nuanced behaviors underscores its value in
577 simulating the real-world dynamics of pesticide fate and transport in Ag-MAR systems.

578 **4.4 Implications for Ag-MAR practice and future research**

579 The three profiles had the same land use and hydroclimatological conditions, yet they
580 varied in the subsurface hydrogeology. Consequently, this study offers valuable insights into
581 the impacts of soil texture and heterogeneity on groundwater recharge and pesticide leaching
582 that may be encountered when implementing Ag-MAR.

583 In terms of groundwater recharge and pesticide residue leaching, P2 (the soil pro
584 with the highest sand content) tended to facilitate preferential flow, leading to faster water

585 flow and pesticide transport (by about 42%) and increased recharge rates (by approximately
586 8%). These conditions also resulted in greater pesticide leaching due to flooding (by about
587 22%). Therefore, Ag-MAR should be implemented with caution in sandy soils. To reduce
588 this risk, it is recommended to apply pesticides well before any planned recharge activities,
589 giving the soil time to abso
590 Choosing the right type of pesticides also matters. Imidacloprid and thiamethoxam, are more
591 likely to leach into groundwater, especially in sandy soils. In cont
592 *chlorantranilip* and *ethoxyfen*, which are less mobile and break down m
593 easily, pose a lower risk.
594 For oxygen (O_2) levels (Figs. S7-S9) during Ag-MAR flooding, there were noticeable
595 sharp drops especially for shallow layers at P1 and P3, wh
596 accumulation at shallow
597 mentioned in . These significant reductions of O_2 le
598 development of anaerobic conditions, which could po
599 Correspondingly, P1 and P3 also had more reduced oxidative environments (lower
600 (ORP) levels than P2 during Ag-MAR (Figs. S7-S9).
601 There were significant electrical conductivity (EC) spikes (even higher than irrigation
602 water) at P3 during Ag-MAR, which highlighted a faster soil salt leach
603 groundwater salinization risk. These ions could originate from the mobilization and release
604 of fertilizer or pesticide residue in the topsoil. P2 and P1 also presented EC spikes, but in
605 general lower than irrigation water and to a lesser extent than P3, suggesting some issu
606 with salt leaching and groundwater salinization but potentially more manageable.
607 In all, each profile illustrated different challenges and opportunities for grou
608 recharge, environmental protection, and agricultural productivity. Tailo
609 practices to the specific conditions reflected in these profiles can balance these aspects.
610 While this study provides valuable insights, it is important to recognize its limitations.
611 The reliance on HYDRUS-1D models, though robust, does not captur
612 dimensional complexity of water and solute movement in the field. Additionally, the study

focused on a limited set of pesticides, which may not represent the full range of behaviors exhibited by other chemicals under similar conditions. Future research should aim to expand the scope of pesticides studied and explore the use of three-dimensional models to capture more detailed spatial variations in Ag-MAR systems.

5 Conclusions

This study emphasized the significant role of soil textu influencing the fate and transports of pesticides in the vadose zone managed aquifer recharge (Ag-MAR) through detailed field experiment modeling using both single and dual-porosity models in HYDRUS-1D. Based on these water flow and pesticide transport information, the suitability of implementi evaluated by combining other biogeochemical indicators inclu reduction potential, and electrical conductivity levels in soil water.

The sandier profiles (P2) demonstrated more pronounced preferential flow, faster water flow, higher groundwater recharge efficiency, but also more soil pesticide and salt leaching correlating with increased ris choosing less mobile pesticides (e.g., *chlorantraniliprole and methoxyfenozide*) and extending the time interval between the last pesticide application and the Ag-MAR e are important for reducing groundwater pollution risks. In contrast textures (P1) showed less preferential flow, slower water flow, lower groundwater recharge efficiency, but raised concerns about the accumula elongate anaerobic conditions in upper soil layers due to capillary barriers, which could severely impact soil growth.

Our results underscore the necessity of considering soil heterogeneity and implementing site-specific management practices in the design and operation of Ag-M maximize groundwater recharge while minimizing environmental risks. Further study calls for the integration of more advanced models that can adequately ca

complex processes of pesticide fate and transports, suc
nonequilibrium processes. On the other hand, the relative
flow/transport and lateral flow remains to be distinguished.

Acknowledgments

We acknowledge Mr. Don Cameron of Terranova Ranch for their support
collecting original data. This work was partially funded by USDA NIFA (Award # 2021-68012-35914), USDA NRCS (grant no NR203A750023C017), the Gordon and Betty Moore Foundation (grant no. 7975), and the California Departmen
(Agreement 17-C0099).

References

Bachand, P.A.M., Roy, S.B., Choperena, J., Cameron, D., and Horwath, W.R., (2014), Implications of using on-farm flood flow capture to recharge groundwater and mitigate flood risks along the Kings River, CA. *Environ. Sci. Technol.*, *48*(23), pp. 13601-13609, doi:10.1021/es501115c

Brunetti, G., Šimůnek, J., and Piro, P., (2016), A comprehensive
analysis of the hydraulic
Journal of Hydrology, *540*, pp. 1146-1161, doi:10.1016/j.jhydrol.2016.07.030

Brunetti, G., Šimůnek, J., Turco, M., and Piro, P., (2017),
surrogate-based modeling for the numerical analysis of Low Impact Develop
techniques, *Journal of Hydrology*, *548*, pp. 2
doi:10.1016/j.jhydrol.2017.03.013

Brunetti, G., Stumpp, C., and Šimůnek, J., (2022), Balancing exploitation and exploration: A novel hybrid global-local optimization stra
model calibration, *Environmental Modelling*, *151*, 1
doi:10.1016/j.envsoft.2022.105341

Czapar, G.F., Horton, R., and Fawcett, R.S., (1992),
TRACER MOVEMENT IN SOIL COLUMNS CONTAINING AN ARTIFICIA
MACROPORE, *J. Environ. Qual.*, *21*(1), pp.
doi:10.2134/jeq1992.00472425002100010016x

Dahlke, H.E., LaHue, G.T., Mautner, M.R.L., Murphy, N.P., Patterson, N.K.
Waterhouse, H., Yang, F.F., and Foglia, L., Managed Aquifer Recharge as a Tool to Enhance Sustainable Groundwater Management in California: Examples From Field and Modeling Studies, In Advanced Tools for I
Management, Friesen, J., RodriguezSinobas, L. (Eds.),
Pollution Environmental Management and Protection, Academic Press Ltd-Elsevier Science Ltd, London, pp. 215-275, doi:10.1016/bs.apmp.2018.07.003, 2018.

de Vries, J.J., and Simmers, I., (2002), Groundwater recharge: an overview of processes *Hydrogeology Journal*, doi:10.1007/s10040-001-0171-7

Dusek, J., Dohnal, M., Snehota, M., Sobotkova, M., Ray, C., and Vogel, (2015), Transport of bromide and pesticides through an undisturbed soil column: A modeling study with global optimization analysis. *J. Contam. Hydrol.*, *175*, pp. 1-16, doi:10.1016/j.jconhyd.2015.02.002

Guo, Z., Fogg, G.E., Chen, K., Pauloo, R., and Zheng, C., (2023), Sustainability of regional groundwater quality in response *Water Resources Research*, *59*(1), pp. e2021WR031459,

Gupta, H.V., Kling, H., Yilmaz, K.K., Decomposition of the mean squared error and NSE performance criteria: Implications for improving hydrological modelling. *Journal of Hydrology*, *377*(1-2), pp. 80-91, doi:10.1016/j.jhydrol.2009.08.003

Haws, N.W., Rao, P.S.C., Šimůnek, J., and Poyer, I.C., (2005), Single-porosity and dual-porosity modeling of water flow and solute transport in subsurface-drained fields using effective field-scale parameters. *Journal of Hydrology*, *313*(3-4), pp. 257-273, doi:10.1016/j.jhydrol.2005.03.035

Holbak, M., Abrahamsen, P., and Diamantopoulos, E Preferential Water Flow and Pesticide Leaching to Drainpipes: The Effect of Drain-Connecting and Matrix-Terminating Biopores. *Water Resources Research*, *58*(7), pp. 21, doi:10.1029/2021wr031608

Imig, A., Augustin, L., Groh, J., Putz, T., Elsner, M., Einsiedl, F., and Rein, A., (2023a), Fate of herbicides in cropped lysimeters: 2. Lea herbicides considering diff *Vadose Zone Journal*, pp. 14, doi:10.1002/vzj2.20275

Imig, A., Augustin, L., Groh, J., Pütz, T., Zhou, T., Einsiedl, F., and Rein, A., (2023b), Fate of herbicides in cropped lysimeters: 1. Influence of different processes and model structure on vadose zone flow. *Vadose Zone Journal*, pp. e20265,

Knoben, W.J.M., Freer, J.E., and Woods, R.A., (2019), Technical note: Inherent benchmark or not? Comparing Nash-Sutcliffe and Kling-Gupta effi *Hydrology and Earth System Sciences*, *23*(10), pp. 4323-4331, doi:10.5194/hess-23-4323-2019

Köhne, J.M., Köhne, S., and Šimůnek, J., (2006), Multi-p transport in structured soil columns *J. Contam. Hydrol.*, *85*(1-2), pp. 1-32, doi:10.1016/j.jconhyd.2006.01.001

Köhne, J.M., Köhne, S., and Šimůnek, J., (2009) applications for *J. Contam. Hydrol.*, *104*(1-4), pp. 36-60, doi:10.1016/j.jconhyd.2008.10.003

Lamontagne, J.R., Barber, C.A., and Vogel, R.M., (2020), Improved Estimators of Model Performance Effi *Water Resources Research*, *56*(9), pp. 25, doi:10.1029/2020wr027101

Levintal, E., Huang, L., García, C.P., Coyotl, A., Fidelibus, M.W., Horv
W.R., Rodrigues, J.L.M., and Dahlke, H.E., (2
agricultural managed aquifer recharge: Linking plant respon
geochemical processes. *Science of the Total Environment*, *864*, pp. 161206,

Levintal, E., Kniffin, M.L., Ganot, Y., Marwaha, N., Murphy, N.P., and Dahlke, H.E., (2023b), Agricultural managed aquifer recharge (Ag-M
sustainable groundwater management. *Crit. Rev. Environ.*
Technol., *53*(3), pp. 291-314, doi:10.1080/10643389.2022.2050160

Lucier, G., and Jerardo, A., 2006. Vegetables and melons outlook. VGS-317, US Department of Agriculture, Economic Research Service.

Mottes, C., Lesueur-Jannoyer, M., Le Bail, M., and Malézieux.
Pesticide transfer models in crop
Agron. Sustain. Dev., *34*(1), pp. 229-250, doi:10.1007/s13593-013-0176-3

Murphy, N.P., Waterhouse, H., and Dahlke, H.E
agricultural managed aquifer recharge on nitrate transport: The role of soil texture and flooding frequency. *Vadose Zone Journal*, *20*(5), pp. 16, doi:10.1002/vzj2.20150

Pang, L.P., Close, M.E., Watt, J.P.C., and Vincent, K.W., (2000), Simulation of picloram, atrazine, and simazine leaching through two New Zealand soils and int
groundwater using HYDRUS-2D. *J. Contam. Hydrol.*, *44*(1), pp. 19-46, doi:10.1016/s0169-7722(00)00091-7

PCPA, 1985.

Perez, N., Singh, V., Ringler, C., Xie, H., Zhu, T.J., Sutanudjaja, E
Villholth, K.G., (2024), Ending groundwater overdra
security. *Nat. Sustain.*, pp. 14, doi:10.1038/s41893-024-01376-w

Radcliffe, D.E., and Šimůnek, J., Soil physics with HYDRUS: Modeling a
applications, CRC Press, pp., 2018.

Ray, C., Vogel, T., and Dusek, J., (2004), Modeling depth-variant and domain-specific sorption and b
J. Contam. Hydrol., *70*(1-2), pp. 63-87, doi:10.1016/j.jconhyd.2003.08.009

Scorza, R.P., and Boesten, J., (2005), Simulation of pesticide le
cracking clay soil with the PEARL model. *Pest Manag. Sci.*, *61*(5), pp. 432-448, doi:10.1002/ps.1004

Shi, Y.H., and Eberhart, R., A modifie
IEEE Inter
Computation, Ieee, Anchorage, Ak, pp. 69-73, doi:10.1109/icec.1998.699146, 1998.

Sidoli, P., Lassabatere, L., Angulo-Jaramillo, R., a
Experimental and modeling of the unsaturated transports of S-metolachlor a
metabolites in glaciofluvial vadose zone soils. *J. Contam. Hydrol.*, *190*, pp. 1-14, doi:10.1016/j.jconhyd.2016.04.001

Šimůnek, J., van Genuchten, M.T., and Sejna, M., (2016), Recent developments and applications of the H
Vadose Zone Journal, *15*(7), pp. 25, doi:10.2136/vzj2016.04.0033

Šimůnek, J., Wendroth, O., Wypler, N., and van Genuchten, M.T., (2001), Non-equilibrium water flow characterized by means of upward infiltration experimen *Eur. J. Soil Sci.*, *52*(1), pp. 13-24, doi:10.1046/j.1365-2389.2001.00361.x

Stagnitti, F., Parlange, J.-Y., Steenhuis, T.S., Boll, J., Pivetz, B., and Barry, D., Transport of moisture and solutes in the unsaturated zone by preferential flo Environmental hydrology, Springer, pp. 193-224, 1995.

Tingle, C.C.D., Rother, J.A., Dewhurst, C.F., Lauer, S Fipronil: Environmental Fate, Ecotoxicology, and Human Reviews of Environmental Contamination and Toxicology: Continuation of Residue Reviews, Ware, G.W. (Ed.), Springer New York, New Y doi:10.1007/978-1-4899-7283-5_1, 2003.

Tudi, M., Ruan, H.D., Wang, L., Lyu, J., Sadler, R., Connell, D., Chu, C., and Phung, D.T., (2021), Agriculture Development, Pesticide Application and Its Impact on the Environment. *Int. J. Environ. Res. Public Heal* 18(3) doi:10.3390/ijerph18031112

Waskom, R., (1995), Best management practices for agricultural pesticide use.

Waterhouse, H., Bachand, S., Mountjoy, D., Choperena, J., Bachand, P.A.M., Dahlke, H.E., and Horwath, W.R., (2020), Agricultural managed aquifer recharge - water quality factors. *Calif. Agric.*, *74*(3), pp. 144- doi:10.3733/ca.2020a0020

Zhou, T., Levintal, E., Brunetti, G., Jordan, S., Harter, T., Kisekka, I., Šimůnek, J., and Dahlke, H.E., (2023), Estimating the impact of vadose zone heterogeneity on agricultural managed aquifer recharge: A combined experimen study. *Water Res.*, *247*, pp. 120781, doi:https://doi.org/10.1016/j.watres.2023.120781

Zhou, T., Šimůnek, J., Braud, I., Nasta, P., Brunetti, G., and Liu, Y., (2022), The impact of evaporation fractionation on the inverse estimation of soil hydraulic an isotope transport parameters. *J. Hydrol.*, *612*, pp. 12810 doi:https://doi.org/10.1016/j.jhydrol.2022.128100